

Magnetic Field Distribution in Solenoids and Circular Coils

Călina Burciu

November 2024

Abstract

For one coil configuration ($r^2 = 0.9898$), the theoretical z-th for half of the magnetic field is $|z_{th}| = 52.11 \cdot 10^{-3}m$ and experimental $|z_{exp}| = (51.04 \pm 0.5) \cdot 10^{-3}m$. The regions of less than 5% deviation for the Helmholtz coil configuration vary between theoretical and experimental results for different coil separations d . For $d = R/2$, ($r^2 = 0.9856$), the theoretical region spans $z'_{th} = \pm 15.40$ mm, giving a total region of $R_{th} = 30.80$ mm, while the experimental region is $z'_{exp} = \pm (10.0 \pm 0.5)$ mm, resulting in a total region of $R_{exp} = (20.0 \pm 1.0)$ mm. At $d = R$, ($r^2 = 0.9714$), the theoretical region expands to $z'_{th} = \pm 35.67$ mm with a total of $R_{th} = 71.34$ mm, whereas the experimental region is $z'_{exp} = \pm (20.0 \pm 0.5)$ mm, yielding a total of $R_{exp} = (40.0 \pm 1.0)$ mm. For the largest separation, $d = 2R$, ($r^2 = 0.8160$), the theoretical region is $z'_{th} = \pm 23.54$ mm, totaling $R_{th} = 47.08$ mm, and the experimental region spans (-10.0 ± 0.5) mm to $+(20.0 \pm 0.5)$ mm, giving a total of $R_{exp} = (30.0 \pm 1.0)$ mm.

1 Introduction

This report explores the magnetic field distribution of two main inductive components; the flat coil and the solenoid, with the aim of examining the physical behavior of the magnetic field generated when a constant current I flows through them and comparing measured data with theoretical literature models. For the solenoid, the goal is to compare with theoretical literature along the center axis of the solenoid and examine the behavior of theoretical and experimental results along the end points of the solenoid. The use of flat coils in this report is to examine the behavior of the magnetic field distribution along its center axis for a single and two coils setup. As well as investigated points of interest along the central axis of the coils such as the point of $\frac{1}{2}B_z^{max}$. Additionally, nature of the magnetic induction is examined along the central axis of the Helmholtz coils to, then be compared with theoretical values along the central axis as well as in a region surrounding the setup's central value. Within each section this report is separated into three tasks reflecting the different apparatus and investigations performed to gain a more comprehensive understanding of the nature of a induced magnetic field.

2 Theoretical Basis

2.1 Magnetic field distribution in a solenoid

To examine the magnetic field distribution of a solenoid with a constant DC current through it, with this in mind the magnetic field distribution can be determined through use of the Ampère-Maxwell equation [?]:

$$\oint \vec{H} \cdot d\vec{l} = \iint \vec{j} \cdot d\vec{A} \quad (1)$$

Where:

$$\vec{H} = \text{Magnetic field intensity} \left(\frac{A}{m} \right)$$

$$\vec{j} = \text{Current Density} \left(\frac{A}{m^2} \right)$$

Given the use of this Eq. 1 within the scope of the first experimental investigation pertains to solenoids and coils. The solution to Eq.1 obtained under the Bio-Savart Law is [?]:

$$d\vec{H} = \frac{I}{4\pi} \frac{d\vec{l} \times \hat{r}}{|\vec{r}|^2} \quad (2)$$

Where:

I = Current (A)

\vec{r} = Position Vector(m)

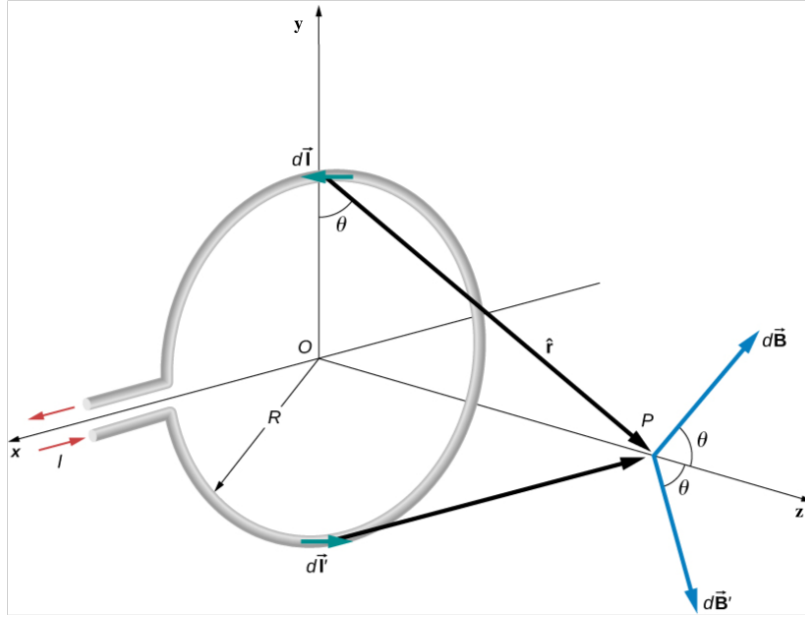


Figure 1: Single loop vector diagram *Source: [?]*

With a lack of a magnetic core the magnetic intensity \vec{H} can be interchanged with the magnetic field \vec{B} through the simple relation:

$$\vec{B} = \mu_0(\vec{H} + \vec{M}), \vec{M} = 0 \implies \vec{B} = \mu_0\vec{H} \quad (3)$$

Where:

\vec{B} = Magnetic Field (T)

μ_0 = Permeability of Free Space ($\frac{N}{A^2}$)

\vec{M} = Material Magnetization ($\frac{A}{m}$)

The magnetic field distribution in the single loop along the axial line \hat{z} from Fig. 1 and Eqs. 2, 3 is thus given as:

$$dB_z = \frac{\mu_0 I}{2} \frac{1}{(R^2 + (z - z')^2)^{\frac{3}{2}}} \quad (4)$$

Where:

$$B(z) = \text{Magnetic Field along } z \text{ (T)}$$

$$R = \text{Radius of Loop (m)}$$

Eq. 4 is limited to the a single loop, however a solenoid persists over many loops over the total length of the solenoid. to determine the magnetic field as a function of z over the length of a solenoid Eq.4 is manipulated to introduce a turn density coefficient, (n) and the integral with respect to z' is taken over the total length L [?]

$$B(z) = \frac{\mu_0 I n}{2} \left[\frac{z}{\sqrt{R^2 + z^2}} + \frac{L - z}{\sqrt{R^2 + (L - z)^2}} \right] \quad (5)$$

Where:

$$n = \text{Turn density } \left(\frac{\text{turns}}{m} \right)$$

$$L = \text{Length of solenoid (m)}$$

2.2 Magnetic Field in a Flat Coil

For a flat coil with N turns of wire, the law can be applied by summing the contributions of all turns. To calculate the magnetic field along the axis of the loop (not just at the center), the Biot-Savart law gives [?]:

$$B_z = \frac{\mu_0 I R^2}{2(R^2 + z^2)^{3/2}} \quad (6)$$

Where:

$$z = \text{Distance from the center of the loop along its axis(m)}$$

$$R = \text{Radius of the Loop(m)}$$

For a single circular loop of radius R , carrying current I , the magnetic field at the center of the loop (or a point on its axis) is:

$$B = \frac{\mu_0 I}{2R}, \text{ for } z = 0 \quad (7)$$

If the flat coil has N turns, the total magnetic field is approximately N times the field produced by a single loop, assuming the turns are closely packed and lie in the same plane. Thus, the field at the center of the coil becomes [?]:

$$B = N \frac{\mu_0 I}{2R} \quad (8)$$

Where:

$$N = \text{Number of turns}$$

Along the axis, the field is:

$$B_z = \mu_0 I N \frac{R^2}{2(R^2 + z^2)^{3/2}} \quad (9)$$

2.3 Magnetic Field in Two Flat Coils

Using Eq. 9, the magnetic field created by two flat coils can be calculated by adding the fields of the single coils. For Helmholtz configuration, the current direction is the same for both coils, with a distance a between them. The formula of magnetic field at the center point with distance d between the coils is [?]:

$$B = \frac{\mu_0 I N R^2}{2} \left[\frac{1}{[R^2 + (z - \frac{a}{2})^2]^{3/2}} + \frac{1}{[(R^2 + (z + \frac{a}{2})^2]^{3/2}} \right] \quad (10)$$

3 Tasks

3.1 Task I

3.1.1 Experiment Setup

To measure the magnetic induction using the MLX90393 sensor, the experimental setup begins with fixing the flat coil to a support stand, ensuring that it is oriented horizontally. The coil has N number of turns and a radius R . The power supply is then connected to the coil, placed in series to measure the current I passing through it, as fig. 2 shows. The MLX90393 magnetic field sensor is fixed on a separate support, positioned near the coil at various distances, along the coil's axis to measure the magnetic field strength along coil's center. The sensor is connected to Arduino GUI, which is used to collect and display the magnetic field data. For this setup, the sensor is moved and **not** the coil, collecting measurements of the magnetic field. As the current is constant, the sensor measures the magnetic field at these different positions, providing data that can be used to analyze the relationship between distance from the center of the coil and magnetic field strength at those points.

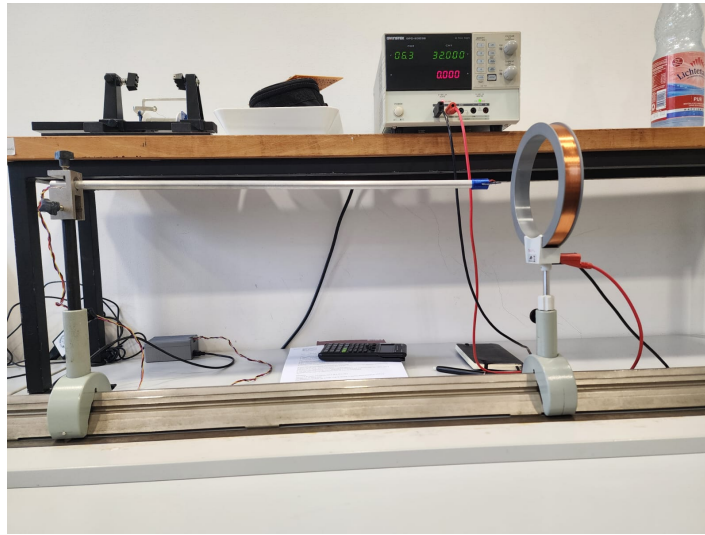


Figure 2: Setup for one Flat Coil

Initial conditions are:

$$\mu_0 = \text{Permeability of free space} = 4\pi \times 10^{-7} \text{N/A}^2$$

$$I = \text{Current through the wire} = (1 \pm 0.0035) \text{A}$$

$$R = \text{Radius of the Coil} = 68 \cdot 10^{-3} \text{m}$$

$$N = \text{Number of turns} = 320$$

The coordinate system is chosen so it can simplify the analysis as much as possible. The sensor is measuring all the components of the magnetic field of the setup, but the focus is set on y-component corresponding to the z-axis of the coil. The origin is set at the center of the coil, going from -0.1 to 0.1 m on z-axis. The results of this experimental data was then compared with theoretical results determined by Eq. 9.

3.1.2 Data Analysis

Fig. 3 present the graphs of calculated and measured values for magnetic induction along z-axis. Over an interval of 0.2 m the magnetic field is consistent and follows the expected theoretical pattern. The values have an uncertainty that fits most of the measured values and $r^2 = 0.9898$. Both of graph reach maximum at $z = 0$, showing good precision on the choice of coordinate system. For the graph of measured values, an average uncertainty for physical measurements and other factors, such

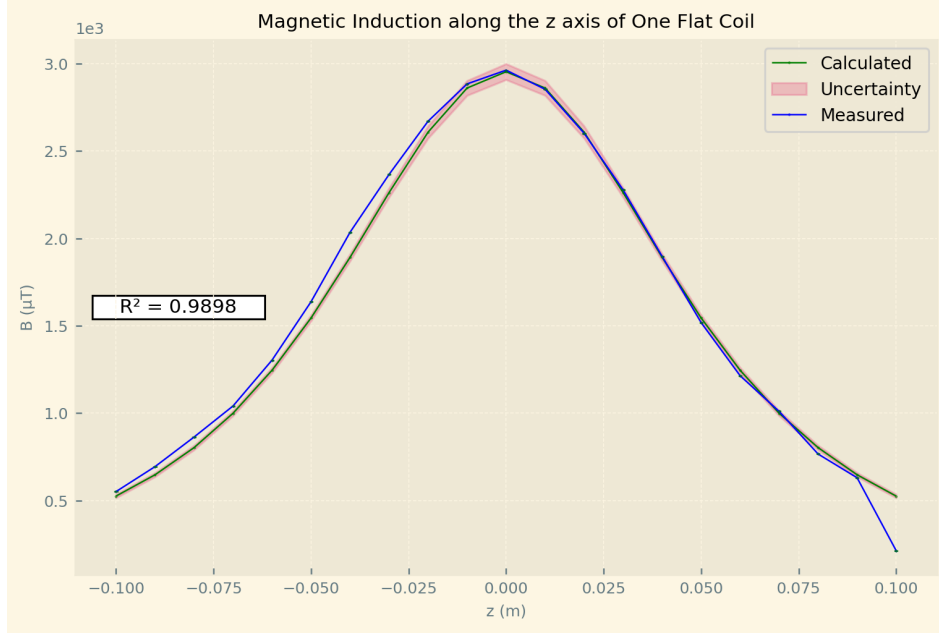


Figure 3: Magnetic Induction of a Flat Coil

as precision of the instrument, the environment. It is also of note that the measurement error in z is $\pm 0.25 \cdot 10^{-3}m$. The positions along the z -axis wherein $B(z)$ is half its maximum value were determined to be $|z_{th}| = 52.11 \cdot 10^{-3}m$ and $|z_{exp}| = (51.04 \pm 0.5) \cdot 10^{-3}m$ for the theoretical and experimental results respectively.

3.2 Task II

3.2.1 Experiment Setup

For the next task, the experimental setup begins by mounting two identical flat coils on a support stand, ensuring they are aligned horizontally and positioned symmetrically, as fig. 4 shows. The second coil is added to the previous experimental setup. The coils are arranged so that the distance between their centers is d , with the power supply connected to both coils, in series, to ensure current flow in the same direction. Their half of distance d represents the new origin of the same coordinate system used in the second experiment.

This experiment investigated three different values of $d = \frac{R}{2}, d = R, d = 2R$ moving the sensor along the z -axis of the two coils from $z = -0.1m$ to $0.1m$ in $0.01m$ intervals. As the current remains constant, the Helmholtz coils setup has the current **I in the same direction**, providing data that can be used to analyze how the magnetic field strength varies with the distance d . The experimental data collected over each value of d , was compared to its respective theoretical values as determined by Eq. 10.

3.2.2 Data Analysis

For $d = \frac{R}{2}$, fig. 5 shows the correlations between the measured and calculated data along the z -axis. Over an interval of $0.01m$, slight deviations are observed between the calculated and experimental results. However, the graphs shows $r^2 = 0.9854$, indicating a strong agreement with the theoretical model. The theoretical region with less than 5% deviation is $z'_{th} = \pm 15.40 \cdot 10^{-3}m$, with a total region of $Reg_{th} = 30.80 \cdot 10^{-3}m$ and the experimental is $\pm(10 \pm 0.5) \cdot 10^{-3}m$, with a total region of $Reg_{exp} = (20 \pm 1) \cdot 10^{-3}m$.

For $d = R$, fig. 6 displays the correlation between theoretical and measured values, with a $r^2 = 0.9714$, demonstrating a slightly higher deviation in comparison to $d = \frac{R}{2}$, but still a close fit to theoretical

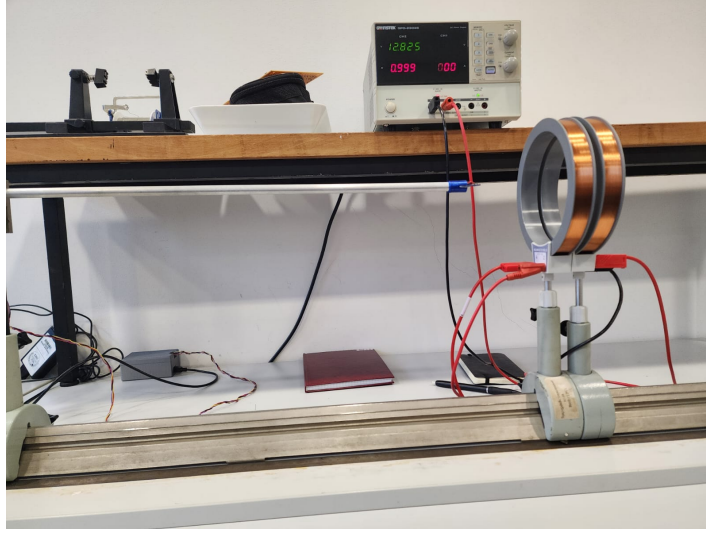


Figure 4: Setup for two Flat Coils at distance $D = R/2$.

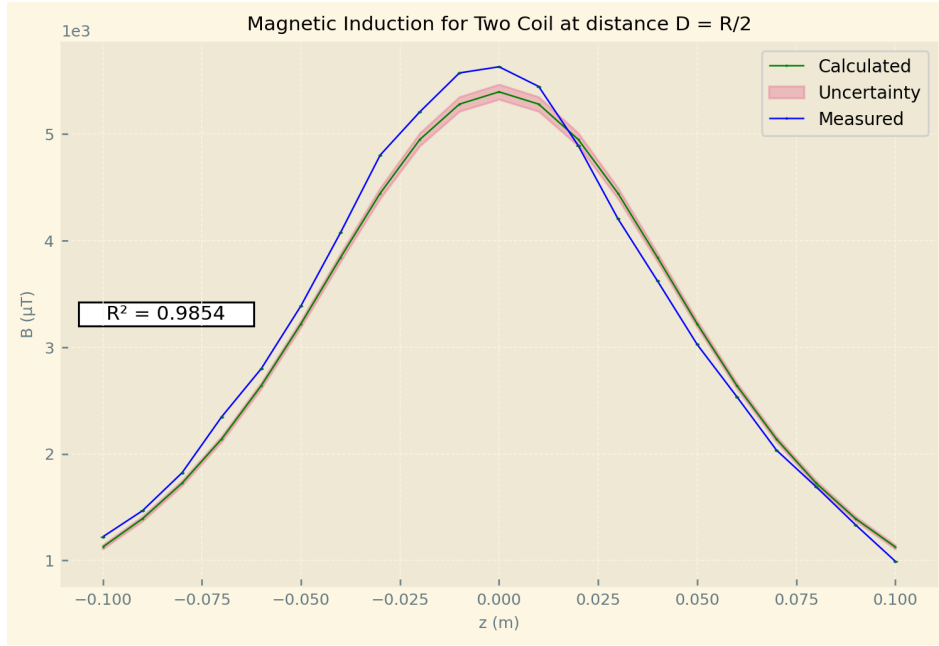


Figure 5: For distance $D = R/2$

data. The theoretical region with less than 5% deviation is $z'_{th} = \pm 35.67 \cdot 10^{-3} m$, with a total region of $Reg_{th} = 71.34 \cdot 10^{-3} m$ and the experimental is $\pm (20 \pm 0.5) \cdot 10^{-3} m$, with a total region of $Reg_{exp} = (40 \pm 1) \cdot 10^{-3} m$.

For $d = 2R$, fig. 7 illustrates the measured versus theoretical magnetic field, showing a lower $r^2 = 0.8160$ than either $d = \frac{R}{2}$ or R , reflecting increased discrepancies as the coil separation distance grows. The theoretical region with less than 5% deviation is $z'_{th} = \pm 23.54 \cdot 10^{-3} m$, with a total region of $Reg_{th} = 47.08 \cdot 10^{-3} m$ and the experimental is from $(-10 \pm 0.5) \cdot 10^{-3} m$ to $(20 \pm 0.5) \cdot 10^{-3} m$, with a total region of $Reg_{exp} = (30 \pm 1) \cdot 10^{-3} m$.

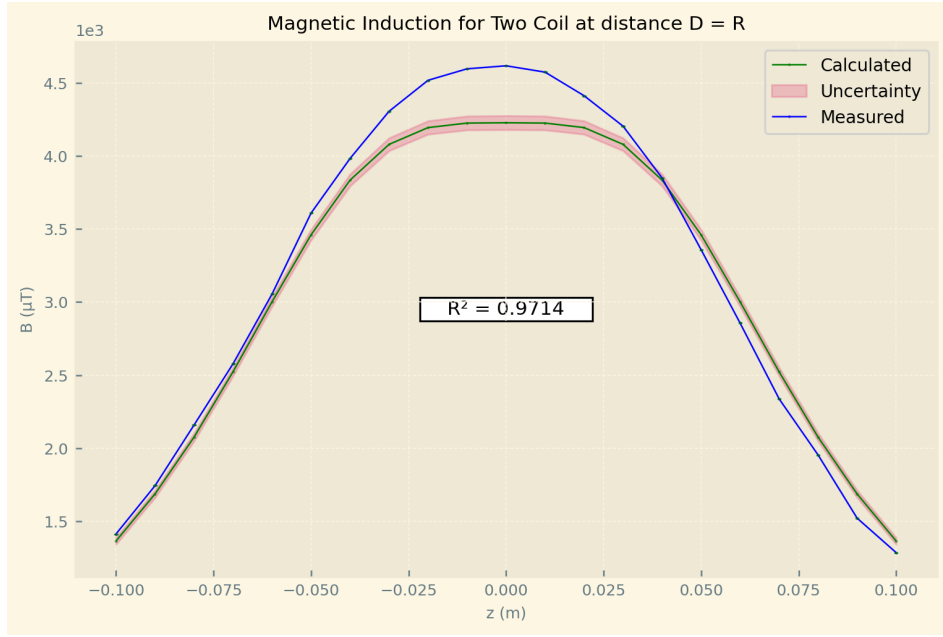


Figure 6: For distance $D = R$

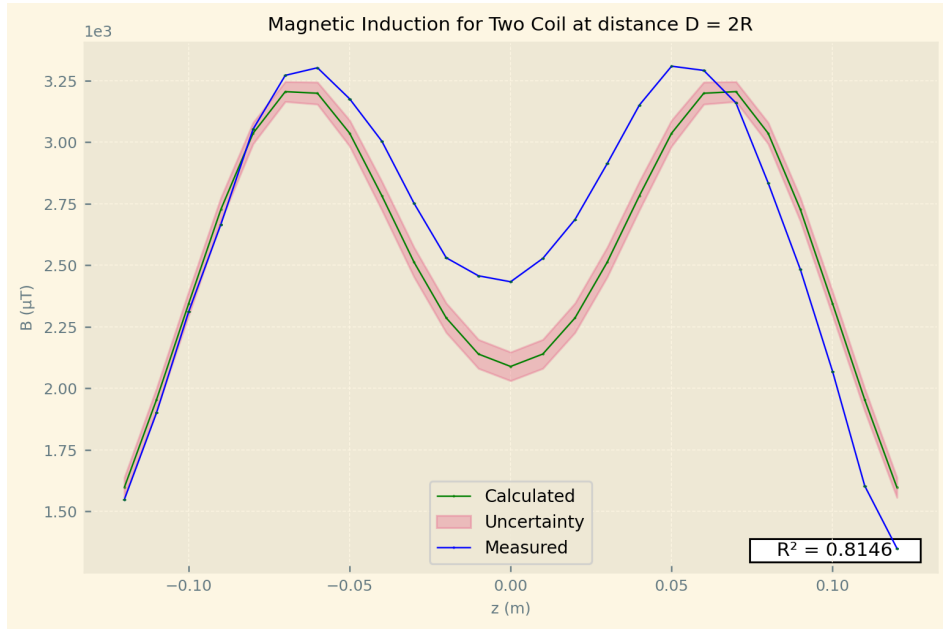


Figure 7: For distance $D = 2R$

4 Discussion

For the first task, the experimental setup and the measurements provide valuable information about the relationship between the magnetic field and distance from the center of the coil.

As the Fig.3 is analyzed, the difference between the calculated and measured values mostly fits the experimental uncertainty. The graphs capture a coefficient of determination of $r^2 = 0.9898$, indicating a close fit to the expected data.

Although, when analyzing the distance from the central value to the half of the magnetic fields magnitude, the majority of the measured values fall between the uncertainty of the calculated values. However, not all the values fit the uncertainty, suggesting that there might be systematic errors in the

experimental setup or some unaccounted environmental factors, such as stray magnetic fields (from other electronic devices) or temperature fluctuations were not considered. The magnetic field of the Earth was subtracted from the beginning of the computation. The magnetic field is symmetric about $z = 0$, with both theoretical and experimental graphs peaking at this point. This confirms a proper alignment of the coil and sensor in the chosen coordinate system, as well as the expected behavior of the magnetic field along the axis of a circular coil.

For the second task, the correlation between the theoretical and experimental magnetic field measurements for coils separation distance, d , highlights the model's reliability and its limitations. Each case presents unique characteristics, with deviations increasing as d grows.

For $d = R/2$, the graph is similar to the graph for one coil, but double in magnitude for the values, indicating that the setup works a lot like a single coil with longer length. This is an ideal setup for seeing the key features and advantages of the Helmholtz configuration. The $r^2 = 0.98564$ is indicating a strong agreement with the theoretical values. The theoretical region with less than 5% deviation is $z'_{th} = \pm 15.40 \cdot 10^{-3}m$, corresponding to a total region $Reg_{th} = 30.80 \cdot 10^{-3}m$ and the experimental is $\pm(10 \pm 0.5) \cdot 10^{-3}m$, giving a total experimental range of $Reg_{exp} = (20 \pm 1) \cdot 10^{-3}m$. The proximity of these regions reflects the strong predictive power of the theoretical model for small coil separations. Any discrepancies are likely due to systematic factors, such as minor wrong alignments in the experimental setup or environmental noise.

In fig. 6, the correlation between theoretical and measured values for $d = R$ displays a slightly higher deviation compared to $d = R/2$. The $r^2 = 0.9714$, though slightly lower than that of $d = R/2$, still demonstrates a strong alignment between the data and the model. The theoretical region with less than 5% deviation is $z'_{th} = \pm 35.67 \cdot 10^{-3}m$, with a total region of $Reg_{th} = 71.34 \cdot 10^{-3}m$ and the experimental is $\pm(20 \pm 0.5) \cdot 10^{-3}m$, with a total region of $Reg_{exp} = (40 \pm 1) \cdot 10^{-3}m$.

The last chosen distance is $d = 2R$, the largest coil separation in this report, with $r^2 = 0.8160$, indicating a noticeable drop in the measured accuracy to the theoretical values. The theoretical region with less than 5% deviation is $z'_{th} = \pm 23.54 \cdot 10^{-3}m$, with a total region of $Reg_{th} = 47.08 \cdot 10^{-3}m$ and the experimental is from $(-10 \pm 0.5) \cdot 10^{-3}m$ to $(20 \pm 0.5) \cdot 10^{-3}m$, with a total region of $Reg_{exp} = (30 \pm 1) \cdot 10^{-3}m$.

These results collectively suggest that the accuracy of the Helmholtz configuration diminishes as d deviates further from the ideal configuration, $d = R/2$. The significant decrease in experimental data with the theoretical model indicates that as the coil separation increases, the model's assumptions may no longer explain the physical system's behavior.

With larger coil separations, the magnetic field becomes weaker and less consistent across the z -axis. The field's intensity decreases, leading to greater deviations between calculated and measured values. The regions of agreement (both in the 5% deviation range and in terms of r^2) shrink as d increases. This reflects how the uniformity of the magnetic field diminishes as the coils are separated.